Romanian Reports in Physics **72**, 402 (2020)

CONTRIBUTION OF CHEMICAL INTERFACE DAMPING TO THE SHIFT OF SURFACE PLASMON RESONANCE ENERGY OF GOLD NANOPARTICLES

ANDREI STEFANCU[1,2*], STEFANIA D. IANCU[1,2], LOREDANA F. LEOPOLD[2*], NICOLAE LEOPOLD[1*]

[1] "Babes-Bolyai" University, Faculty of Physics, Cluj-Napoca, Romania
[2] University of Agricultural Sciences and Veterinary Medicine, Faculty of Food Science and Technology, Cluj-Napoca, Romania
[*] Corresponding author: *stefancu.andrei16@gmail.com; loredana.leopold@usamvcluj.ro; nicolae.leopold@phys.ubbcluj.ro*

Received October 21, 2019

Abstract. The effects that determine the shift and damping of the surface plasmon resonance (SPR) band of colloidal gold nanoparticles due to the chemisorption of tetrahydroxyborate ($B(OH)_4$) anions are analyzed experimentally and theoretically. The contribution of chemical interface damping, change in refractive index and charge density variations to the experimentally observed shift of the SPR band are evaluated qualitatively by simulating the optical response of gold nanoparticles upon the chemisorption of $B(OH)_4$ anions. The results show that changing the refractive index of the medium and the charge density cannot account entirely for the shift of the SPR band. Thus, chemical interface damping should be considered when analyzing surface effects in the presence of strongly chemisorbed adsorbates.

Key words: gold nanoparticles; chemical interface damping; Drude model; surface plasmon resonance.

1. INTRODUCTION

Optical properties of plasmonic structures are of great interest in many nanotechnological applications, but also for understanding surface effects in plasmon–driven catalysis or surface-enhanced Raman scattering. Among the metallic nanoparticles, gold nanoparticles (AuNPs) are the most widely used due to the ease of surface chemical functionalization and increased bioavailability compared to other metallic nanoparticles. Additionally, numerous studies reported the possibility of using the surface of metallic gold or silver nanoparticles (AgNPs) for specific chemical reactions, which represents the holy grail of catalysis – to promote selectively the chemical transformation of a target molecule from a mixture containing multiple analytes [1–3]. Such selective chemical reactions can be achieved due to an additional energy provided by resonantly excited plasmons, energy that can be transferred selectively to chemically adsorbed molecules.

From a rigorous point of view, a plasmon is defined as a quantum quasi-particle representing the elementary excitation, or mode, of the charge density oscillation in

a plasma. However, from the point of view of the optical response of the nanostructure, plasmons can be thought as the electromagnetic modes of the system [4].

After the excitation of plasmons, electron-hole pairs are excited in metallic nanoparticles and their energy decays rapidly, on the order of tens of femtoseconds, due to multiple energy dissipation pathways. Because of the rapid decay of plasmon energy, direct monitoring of this effect is difficult and the homogeneous plasmon resonance band linewidth of nanoparticles, Γ, is used instead [5]:

$$\Gamma = \Gamma_b + \Gamma_{rad} + \Gamma_{surf} + \Gamma_{CID}. \quad (1)$$

The bulk damping, which contributes to the plasmonic linewidth of metallic NPs through the term Γ_b, describes the scattering of electrons with thermal phonons and other defects in the metallic structure and converts the incoming photons into heat. It is usually assumed that bulk damping efficiency of metallic nanoparticles is the same as for bulk material.

The radiation damping, Γ_{rad} describes the damping of the surface plasmon energy by secondary light emission, whereas surface scattering, Γ_{surf} describes the scattering of electrons at the surface of the nanoparticles.

Finally, chemical interface damping (CID), Γ_{CID} describes the damping of the surface plasmon energy by charge transfer to an adsorbate [6]. Therefore, the linewidth, position and intensity of the homogeneous surface plasmon resonance (SPR) extinction band can provide valuable information on the mechanisms that lead to plasmon energy dissipation. The challenge is to minimize all the effects that lead to energy dissipation and to increase the proportion of plasmon energy transferred to chemically attached molecules.

From all the effects that contribute to energy dissipation, CID is the least understood mechanisms and, at the same time, contributes the most in transferring energy to adsorbed molecules. CID avoids the intermediate step of creating the hot electron-hole pairs, instead the plasmon energy decays directly into an interfacial charge transfer state [5, 6]. Thus, CID can be thought as the inelastic scattering of electrons at the surface of the nanoparticles, transferring energy into the available molecular orbitals attached to the surface [7]. Recently, Link *et al.* showed that CID depends inversely proportional to the size of the nanoparticles, which confirms that at least CID determines the interaction of hot electrons with the surface of the nanoparticles, confirming previous work on this matter [6, 7].

However, it is difficult to separate the contribution of CID to energy dissipation of plasmonic energy from all the other mechanisms. Moreover, it is not even clear if CID is a different effect from surface scattering of electrons.

In general, the chemisorption of molecules to the surface of the nanoparticles leads to a myriad of effects such as a change in the refractive index of the embedding medium or a change in the charge density of nanoparticles following the formation of a chemical bond which can be determined experimentally. In this study is shown that a qualitative picture of the energy transferred to the adsorbed molecule through CID can be obtained by monitoring the shift of the SPR energy of AuNPs following

the chemisorption of nucleophilic tetrahydroxyborate anions, $B(OH)_4^-$. It is shown that the changes of the SPR energy following the chemisorption of $B(OH)_4^-$ cannot be explained entirely based on refractive index and charge density variations, therefore CID effects must be taken in consideration.

2. EXPERIMENTAL AND MODELLING METHODS

For the synthesis of AuNPs the citrate reduction method was used. Briefly, in 98 mL ultrapure water 600 µL $HAuCl_4$ solution (2%) was added and the solution was brought to a boil under magnetic stirring. Once the solution was boiling, 2 mL sodium citrate (1%) were added and the solution was boiled for another 30 minutes. All solutions were prepared in ultrapure water with a resistivity higher than 18 MΩ, obtained from a Millipore Direct-Q3 UV purification system. The diameter of the obtained AuNPs was approximated to 11 nm, by using the calculation method provided by Haiss *et al.* [11], based on the ratio between the extinction at resonance energy and extinction value at 450 nm.

For the experimental UV-Vis spectra a Jasco V-630 spectrophotometer and quartz cells with an optical pathway of 1 cm were used.

For the simulation of the extinction spectra, Matlab software, Mathworks, version R2018a was used. The optical properties of metallic nanoparticles were simulated through the boundary element method (BEM) [8].

Two different physical systems presented schematically in Fig. 1 were simulated. For simulating the change in refractive index determined by the adsorbed molecules, a core-shell system, with the core represented by a gold sphere with diameter of 10 nm and a coating layer of $B(OH)_4^-$ with thickness of 1 nm and varying refractive index between 1.33 and 1.45 was modeled [9].

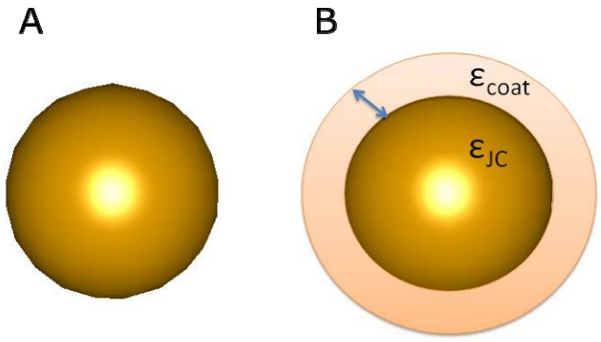

Fig. 1 – Schematic representation of the physical systems used for simulating the optical response of AuNPs: A) gold nanosphere with diameter of 10 nm; B) core–shell system with an inner core of gold of 10 nm diameter and an outer shell of thickness of 1 nm and refractive index determined by the specific chemical nature of the adsorbate. ε_{JC} represents the dielectric function obtained experimentally [10] and ε_{coat} the dielectric function of the adsorbate shell.

For simulating the optical response of AuNPs plotted in Fig. 1, the following intrinsic parameters shown in Table 1 were used.

Table 1

Parameters for calculating the optical properties of AuNPs [4]

Parameter	Value
Nr. of free electrons (N)	5.8×10^{29} m^{-3}
Effective mass (m^*)	0.99
Bulk damping (γ_b)	73 meV
Core polarization (ε_∞)	9.1

3. EXPERIMENTAL RESULTS

The simulated extinction spectrum for individual 10 nm diameter AuNPs reproduces satisfactorily the experimental extinction spectrum, obtained as contributions from all nanoparticles in the solution (Fig. 2A). Despite the heterogeneity of the colloidal nanoparticles the differences between the simulated and experimental spectra are small. The only significant differences are the increased width of the SPR band of the experimental spectrum, as well as a slight blue-shift. Partly, these spectral differences between the experimental and simulated spectra can be attributed to the presence of citrate surfactant.

Next, $NaBH_4$ was added to the gold colloidal solution up to a concentration of 1 mM. It is known that $NaBH_4$ spontaneously hydrolyzes in water, forming tetrahydroxyborate anions [12–14]:

$$BH_4^-(aq) + 4H_2O(l) \rightarrow B(OH)_4^-(aq) + 4H_2(g).$$

It has been shown that $B(OH)_4^-$ has a high affinity for the gold surface, being able to displace citrate anions from the metal surface [15].

Figure 2B shows the UV-Vis extinction spectrum of the colloidal AuNPs obtained by citrate reduction and the extinction spectrum of the same colloid after the addition of $NaBH_4$ 1 mM. The replacement of citrate capping agent on the silver surface by the highly nucleophilic $B(OH)_4^-$, leads to a noticeable shift of 10 nm in the SPR band of AuNPs (Fig. 2B). The shift of the SPR band can be attributed to a myriad of effects, such as charge density variations in the AuNPs, refractive index variations of the surrounding medium and not lastly to CID.

The contributions to the shift of the SPR band of AuNPs can be determined by modelling theoretically the optical response of AuNPs. To describe the dielectric constant of AuNPs, the simple Drude model is used. The dielectric constant of metallic nanoparticles describes the dispersive properties of nanoparticles and the

interaction of metallic nanoparticles with light at different energies. The physical reason for this strong frequency dependence of the dielectric constant is a change in the phase of the induced currents with respect to the driving field for frequencies close to the reciprocal of the characteristic electron relaxation time of the metal. The dielectric constant in the Drude model is given by [16]:

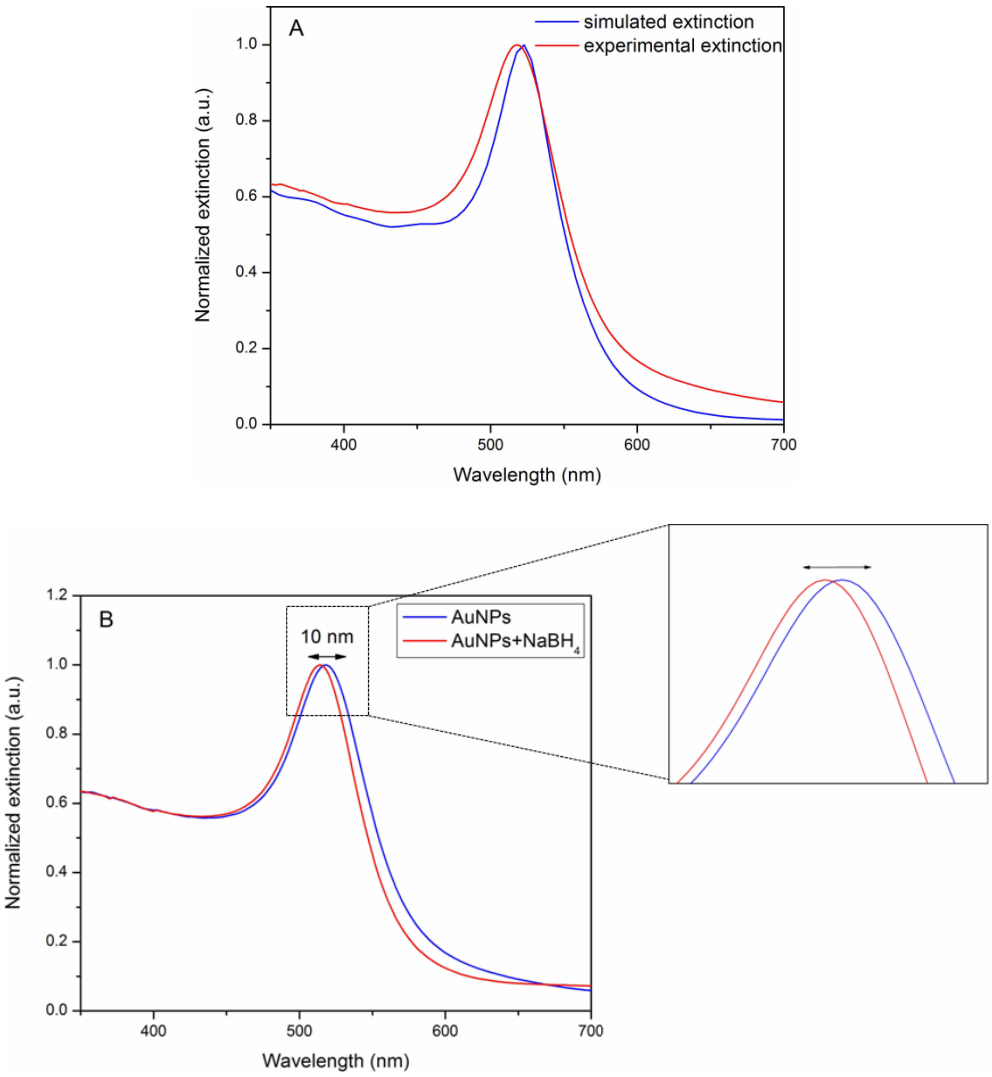

Fig. 2 –A) Simulated and experimental extinction spectra of AuNPs. Three experimental extinction spectra were averaged and both spectra were normalized to unity; B) UV-Vis extinction spectrum of the colloidal AuNPs obtained by citrate reduction and the extinction spectrum of the same colloid after the addition of $NaBH_4$ 1 mM. The shift of the SPR band of AuNPs upon the addition of $NaBH_4$ is highlighted in the right image.

$$\varepsilon_{Drude} = \varepsilon_{\infty} - \frac{\omega_p^2}{\omega^2 + i_{\gamma b}\omega}, \tag{2}$$

where ε_{∞} is the core background polarization created by the ion core of the nanoparticles, γ_b is the damping of the bulk metal and ω_p is the plasma frequency of the metal, given by:

$$\omega_p = \sqrt{\frac{Ne^2}{m^*\varepsilon_0}}, \tag{3}$$

where N is the free electron density, e the elementary charge, m^* the effective mass of charge carriers in the nanoparticles and ε_0 is the electric permittivity of free space. All the parameters used for simulating the extinction spectra of AuNPs are given in Table 1.

In general, the dielectric constant is complex, the imaginary part describing the absorption of light. Figure 3 presents the real and imaginary part of the dielectric function of a 10 nm AuNP obtained from the Drude model (equation (2)) and the experimental dielectric function tabulated by Johnson and Christy [10].

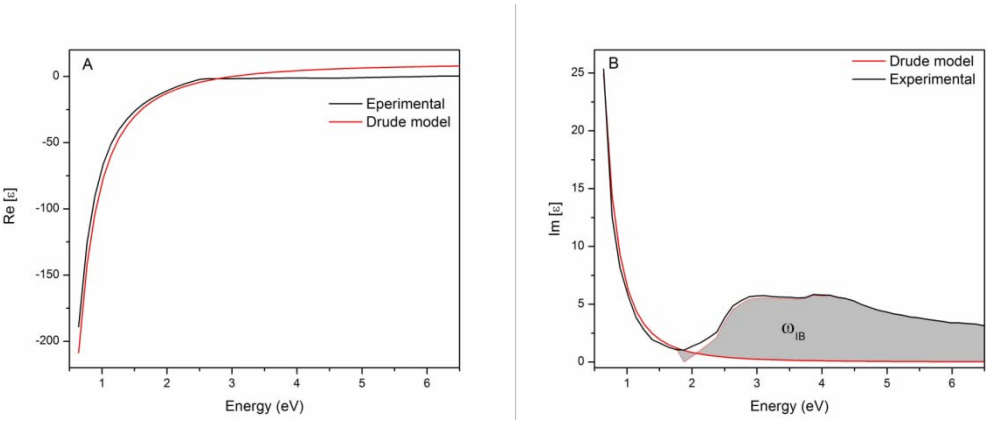

Fig. 3 – The real (A) and imaginary (B) part of the dielectric constant of Au obtained experimentally by Johnson and Christy [10] and simulated on a 10 nm AuNP, based on the Drude model.

As can be observed from Fig. 3, the Drude model yields accurate results for the real part of dielectric constant. However, it does not take into consideration interband transitions, which in gold take place at energies above 1.7 eV and contribute to the imaginary part of the dielectric constant, increasing the absorption [17].

A simple, empirical method to correct the Drude dielectric constant and to account for the interband transitions is to modify the plasma frequency of AuNPs by adding the contribution from interband transition, ω_{IB} (Fig. 1B):

$$\omega_{p,IB} = \omega_{p,Drude} + \omega_{IB}. \quad (4)$$

The *quasi-static* approximation was used until now, which assumes that the nanoparticle is much smaller than the wavelength, such that the electromagnetic fields are constant over the entire volume of the metallic nanoparticles [16]. However, for an accurate description of the optical response of metallic nanoparticles, retardation effects have to be taken into account, which appear due to the finite speed of light such that the electromagnetic fields are slightly different at different points inside nanoparticles. To take this effect into considerations, the full Maxwell's equations for the metallic nanoparticles were solved, which obviously adds to the computation time.

For simulating the retardation effects, the diameters of the gold nanospheres were ranged between 5 and 75 nm and the SPR energy was calculated using the full Maxwell's equations in the BEM method for each diameter. In Fig. 4 the resonance energy variation with increasing diameter of AuNP in the 5–75 nm range is presented.

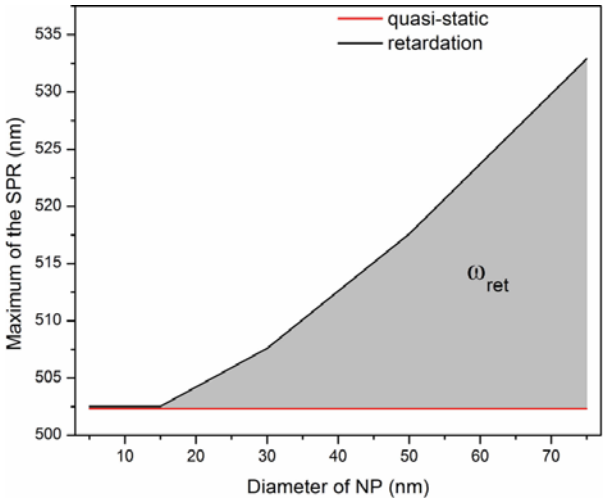

Fig. 4 – Retardation effects on the resonance energy of a AuNP, which depend on the diameter of the nanoparticle, describing the effect of the finite light speed in the metal on the resonance energy.

Therefore, for a complete description of the optical response of AuNPs, the plasma frequency of AuNPs has to be modified again, by adding an additional term representing retardation effects:

$$\omega_{p,IB,ret} = \omega_{p,Drude} + \omega_{IB} + \omega_{ret}. \quad (5)$$

In order to simulate the optical response of AuNPs, the extinction cross section (C_{ext}) of the nanoparticles is defined as the sum of the scattering cross

section (C_{sca}) and the absorption cross section (C_{abs}). The C_{ext} experiences a resonance at the Frohlich condition [16]:

$$C_{ext} = C_{sca} + C_{abs}, \tag{6}$$

with

$$C_{sca} = \frac{k^4}{6\pi}|\alpha|^2 \qquad C_{abs} = k\mathrm{Im}[\alpha]$$

where $k = \frac{2\pi n_{med}}{c}$ is the wavenumber of the electromagnetic wave in the medium with the refractive index n_{med} and α is the polarizability of the AuNP.

Naturally, nucleophilic molecules tend to donate an electron, so the chemisorption of nucleophilic molecules would result in the (partial) charge transfer from the adsorbed molecule to the nanoparticle. In order to distinguish if this effect accounts entirely for the shift of the resonance energy upon $B(OH)_4^-$ chemisorption, the dielectric function of AuNPs was calculated using a modified charge density, ΔN, according to the following procedure [6]:

$$\varepsilon_{\Delta N} = \varepsilon_{JC} - \varepsilon_{Drude}(\omega_p) + \varepsilon_{Drude}(\omega_{p'}), \tag{7}$$

with

$$\omega_p = \sqrt{\frac{Ne^2}{m^*\varepsilon_0}} \tag{8}$$

and

$$\omega_p' = \sqrt{\frac{(N+\Delta N)e^2}{m^*\varepsilon_0}}. \tag{9}$$

The charge density term (N) in equation (9) was modified through the extra term ΔN to determine the influence of charge density variation on the SPR wavelength. Realistically, the charge density should not vary more than 1%, which happens if each adsorbed $B(OH)_4^-$ donates one electron to the AuNP [6]. In this case, the shift of the SPR energy is less than 2 nm (Fig. 5). However, the charge density (N) was varied from 0.5 to 3% to observe the trend of the shift in SPR energy and the resulting extinction spectra was simulated.

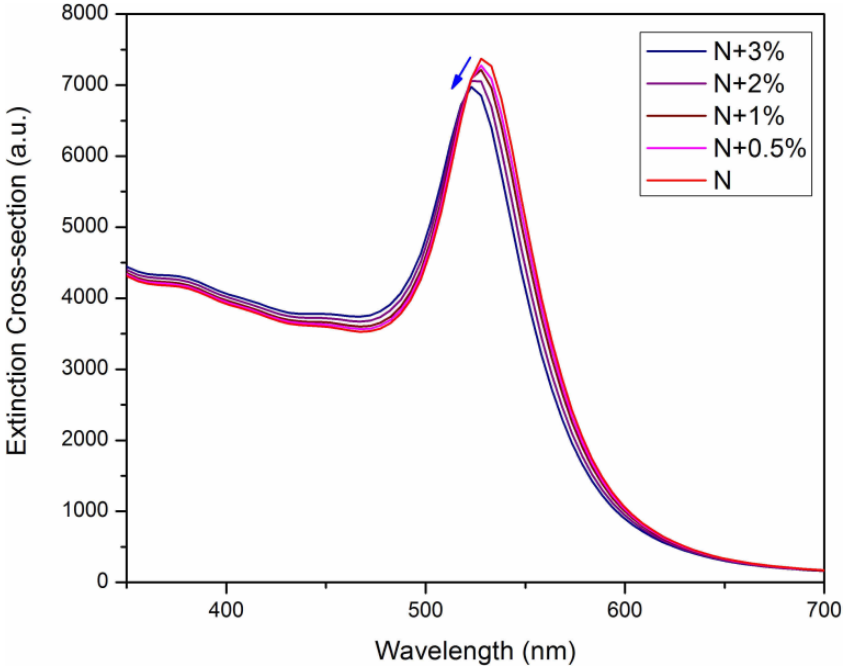

Fig. 5 – Calculated extinction spectra of a 10 nm AuNP for different charge densities. The SPR shifts towards lower wavelengths following an increase in charge density. The shift of the SPR band was lower than 5 nm in the studied interval.

The blue shift of the SPR band can be explained based on the model proposed by Henglein *et al.* using silver colloids [18]. The adsorbed nucleophiles shift the Fermi level of AgNPs towards cathodic potential, increasing the sensitivity of the nanoparticles for electrophilic molecules and lead to the oxidation of AgNPs by electrophilic molecules. For example, they reported the reduction of methyl viologen (MV^{2+}), which took place only after the surface of the nanoparticles was modified by nucleophilic species (CN^-). In the lack of the nucleophilic species, no interaction between MV^{2+} and AgNPs was observed.

The chemisorption of nucleophiles (X) onto AgNPs can be modeled as follows [18]:

$$Ag_nAg + X = Ag^{\delta^-}_{n-1}Ag^{\delta^-}X \qquad \text{(reaction 1)}$$

$$Ag^{\delta^-}_{n-1}Ag^{\delta^+}X \xrightarrow{\text{electrophile}} nAgX \qquad \text{(reaction 2)}$$

In the first step (reaction 1), a nucleophilic molecule donates an electron pair into an unoccupied orbital on the metallic surface, the surface atom acquiring a slight positive charge δ^+ and the inner of the AgNP a corresponding negative

charge δ^-. A certain number of surface atoms are 'pre-complexed' or 'pre-oxidized' by this effect until an equilibrium is reached where the negative charge accumulated inside prevents further electron donation.

In the second step (reaction 2), diffused oxygen in the colloidal solution picks up the excess negative charge of the interior and dissolves the metal as AgX molecules. These changes in the Fermi level of silver colloids are reflected as a shift on the SPR band of the AgNPs.

The decrease and broadening of the SPR band induced by nucleophilic reagents is understood by analyzing equation (1). An increase in the Γ_{CID} leads to a decrease in the coherence of plasmon oscillations, experimentally determined by the half-width of the homogeneous scattering band of AuNPs.

To probe the effect of the change in refractive index of the embedding medium, a core-shell system presented in Fig. 1B was modelled. The $B(OH)_4^-$ anions adsorb on metallic surfaces and form a thin layer with a thickness of approximately 1 nm [9]. Since the refractive index of this adsorbed layer can change comparatively to isolated, free $B(OH)_4^-$, the extinction spectra were simulated by varying the refractive index of the thin layer between 1.33 and 1.45 (Fig. 6).

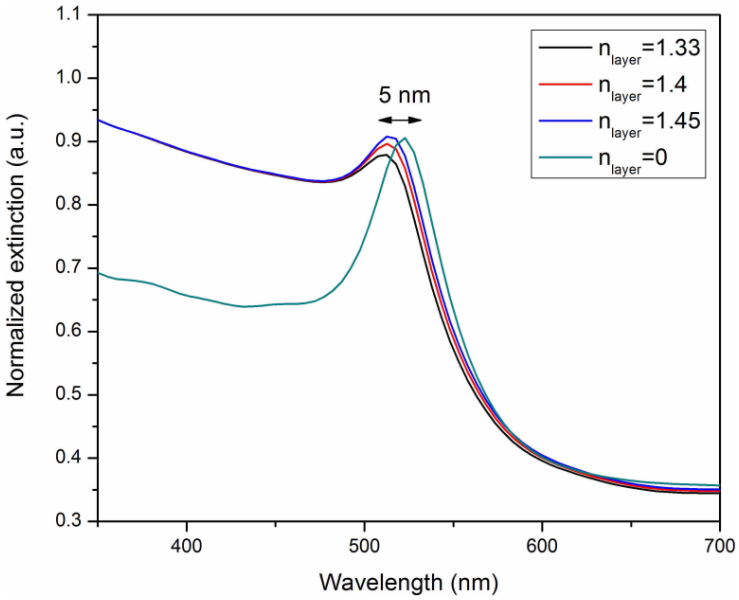

Fig. 6 – Calculated extinction spectra of a 10 nm AuNP using a modified dielectric constant of the surrounding medium, given by the adsorbed $B(OH)_4^-$. The effects of change in refractive index upon chemisorption of $B(OH)_4^-$ simulated with a refractive index between 1.33 and 1.45, which leads to a damp of the SPR band, as well as the shift towards lower wavelengths (higher energies). The maximum shift of the simulated SPR band of AuNP is less than 5 nm.

As can be observed from the Fig. 6, the SPR band shifts towards higher energies with increasing the refractive index of the adsorbed $B(OH)_4^-$ layer. However, the shift observed was not higher than 5 nm in the studied interval.

4. CONCLUSION

Changes in refractive index (ΔRI) and charge density (ΔN) cannot account entirely for the damping and shifting of the SPR energy (ΔE) of AuNPs following the chemisorption of $B(OH)_4^-$ nucleophilic species. Thus, the following qualitative relation can be considered:

$$\Delta E_{\Delta N} + \Delta E_{RI} < \Delta E_{experimental}$$

Therefore, CID should be considered when studying the optical properties of metallic nanoparticles. Moreover, by isolating the CID contributions to the change in the optical properties of AuNPs the amount of energy transferred to adsorbates and the capacity of AuNPs to catalyze specific chemical reactions can be approximated. These results are in line with other studies showing the CID contributions to the shift of SPR energy [2, 3, 19].

Acknowledgements. Financial support from the Romanian Ministry of Research and Innovation, CCCDI-UEFISCDI, project numbers PN-III-P4-ID-PCCF-2016-0112 and PN-III-P1-1.2-PCCDI-2017-0056 within PNCDI III, is highly acknowledged.

REFERENCES

1. Gadzuk, J.W., *Resonance-assisted, hot-electron-induced desorption*, Surface Science **342**(1), 345–358 (1995).
2. Foerster, B., et al., *Plasmon damping depends on the chemical nature of the nanoparticle interface*, Science Advances **5**(3), 2019.
3. Boerigter, C., et al., *Evidence and implications of direct charge excitation as the dominant mechanism in plasmon-mediated photocatalysis.* Nature Communications **7**, 10545 (2016).
4. Le Ru, E.C. and P.G. Etchegoin, *Chapter 3 – Introduction to plasmons and plasmonics*, in *Principles of Surface-Enhanced Raman Spectroscopy*, E.C. Le Ru and P.G. Etchegoin (Editors), 2009, Elsevier, Amsterdam, p. 121–183.
5. Link, S. and M.A. El-Sayed, *Spectral Properties and Relaxation Dynamics of Surface Plasmon Electronic Oscillations in Gold and Silver Nanodots and Nanorods*, The Journal of Physical Chemistry B **103**(40), 8410–8426 (1999).
6. Foerster, B., et al., *Chemical Interface Damping Depends on Electrons Reaching the Surface*, ACS Nano **11**(3), 2886–2893 (2017).
7. Persson, B.N.J., *Polarizability of small spherical metal particles: influence of the matrix environment*, Surface Science **281**(1), 153–162 (1993).
8. Hohenester, U. and A. Trügler, *MNPBEM – A Matlab toolbox for the simulation of plasmonic nanoparticles*, Computer Physics Communications **183**(2), 370–381 (2012).

9. Demetriou, A. and I. Pashalidis, *Adsorption of boron on iron-oxide in aqueous solutions*, Desalination and Water Treatment **37**(1–3), 315–320 (2012).
10. Johnson, P.B. and R.W. Christy, *Optical Constants of the Noble Metals*, Physical Review B **6**(12), 4370–4379 (1972).
11. Haiss, W., et al., *Determination of Size and Concentration of Gold Nanoparticles from UV−Vis Spectra*, Analytical Chemistry **79**(11), 4215–4221 (2007).
12. Pacioni, N.L., et al., *Synthetic Routes for the Preparation of Silver Nanoparticles*, in *Silver Nanoparticle Applications: In the Fabrication and Design of Medical and Biosensing Devices*, E.I. Alarcon, M. Griffith, and K.I. Udekwu (Editors), 2015, Springer International Publishing: Cham, pp. 13–46.
13. Polte, J., et al., *Formation Mechanism of Colloidal Silver Nanoparticles: Analogies and Differences to the Growth of Gold Nanoparticles*, ACS Nano **6**(7), 5791–5802 (2012).
14. Andrieux, J., et al., *Spontaneous hydrolysis of sodium borohydride in harsh conditions*, International Journal of Hydrogen Energy **36**(1), 224–233 (2011).
15. Ansar, S.M., et al., *Removal of Molecular Adsorbates on Gold Nanoparticles Using Sodium Borohydride in Water*, Nano Letters **13**(3), 1226–1229 (2013).
16. Maier, S.A., *Plasmonics: Fundamentals and Applications*, 2007, p. 245.
17. Foerster, B., et al., *Particle Plasmons as Dipole Antennas: State Representation of Relative Observables*, The Journal of Physical Chemistry C **122**(33), 19116–19123 (2018).
18. Linnert, T., P. Mulvaney, and A. Henglein, *Surface chemistry of colloidal silver: surface plasmon damping by chemisorbed iodide, hydrosulfide (SH-), and phenylthiolate*, The Journal of Physical Chemistry **97**(3), 679–682 (1993).
19. Aizpurua, J., et al., *Theory of hot electrons: general discussion*, Faraday Discussions **214**(0), 245–281 (2019).